



Project acronym and title:

**SECURE – Subsurface Evaluation of Carbon capture
and storage and Unconventional risks**

**Report on best practice methods for monitoring induced and
triggered seismicity**

Authors and affiliation:

**Trine Dahl-Jensen, Tine B. Larsen and Peter H. Voss
GEUS**

¹Geological Survey of Denmark and Greenland (GEUS),
Øster Voldgade 10, DK-1350, Copenhagen, Denmark

Email of lead author:

tdj@geus.dk

4.2

Revision:1

Disclaimer

This report is part of a project that has received funding by the *European Union's Horizon 2020 research and innovation programme* under grant agreement number 764531.

The content of this report reflects only the authors' view. The *Innovation and Networks Executive Agency (INEA)* is not responsible for any use that may be made of the information it contains.



Project funded by the European Commission within the Horizon 2020 Programme

Dissemination Level

PU	Public
CO	Confidential, only for members of the consortium (incl. the Commission Services)
CL	Classified, as referred to in Commission decision 2001/844/EC

Deliverable number:	4.2
Deliverable name:	Report on best practice methods for monitoring induced and triggered seismicity
Work package:	WP4
Lead WP/deliverable beneficiary:	GEUS

Status of deliverable		
	By	Date
Submitted (Author(s))	Trine Dahl-Jensen, Tine B. Larsen, Peter H. Voss	May 1, 2020
Verified (WP leader)	Matteo Icardi	May11 2020
Approved (EB member)	Pierre Cerasi	May 11 2020
Approved (Coordinator)	Edward Hough	May 27 2020

Author(s)		
Name	Organisation	E-mail
Trine Dahl-Jensen	GEUS	tdj@geus.dk
Tine B. Larsen	GEUS	tbl@geus.dk
Peter H. Voss	GEUS	pv@geus.dk



Public introduction

Subsurface Evaluation of CCS and Unconventional Risks (SECURE) is gathering unbiased, impartial scientific evidence for risk mitigation and monitoring for environmental protection to underpin subsurface geenergy development. The main outputs of SECURE comprise recommendations for best practice for unconventional hydrocarbon production and geological CO₂ storage. The project is funded from June 2018–May 2021.

The project is developing monitoring and mitigation strategies for the full geenergy project lifecycle; by assessing plausible hazards and monitoring associated environmental risks. This is achieved through a program of experimental research and advanced technology development that includes demonstration at commercial and research facilities to formulate best practice. We will meet stakeholder needs; from the design of monitoring and mitigation strategies relevant to operators and regulators, to developing communication strategies to provide a greater level of understanding of the potential impacts.

The SECURE partnership comprises major research and commercial organisations from countries that host shale gas and CCS industries at different stages of operation (from permitted to closed). We are forming a durable international partnership with non-European groups; providing international access to study sites, creating links between projects and increasing our collective capability through exchange of scientific staff.

Executive report summary

Best practice for monitoring induced and triggered seismicity depends to a high degree on local conditions, but in all cases establishing a high-quality pre-operational baseline is recommended. During operations a local network should be deployed for monitoring and mitigation purposes. If the Traffic Light System is used as a mitigation tool, it is important that the monitoring network has a detection level way below the acceptable level of microseismicity as determined by authorities.

The monitoring network at Stenlille, in operation since summer 2018, has not detected any events within the Stenlille gas storage facility, but did detect other events further away: This makes it possible to estimate the detection level within the gas storage area.



Contents

Public introduction	ii
Executive report summary	ii
Contents	iii
1 Introduction	1
2 The role of baseline monitoring	1
3 Establishing a post-operational baseline	1
4 The Stenlille gas storage facility	2
4.1 The Stenlille post-operational microseismic monitoring network	3
4.2 Data analysis	4
4.3 Detection of events	4
4.4 Correlation with pumping	8
4.5 Detection level	8
5 Discussion of results – why do we not see any events at Stenlille?	9
6 Choosing the optimal network	10
7 Discriminating between natural seismicity and anthropogenic seismicity	10
8 Conclusion	11
9 References	12
Appendix 1	13



FIGURES

Figure 1. The Stenlille gas storage is located on Sjælland (red hexagon), The triangles are seismological stations (green – permanent network stations; yellow – additional Raspberry Shake stations deployed and used in this study)

Figure 2. Cross section of the Stenlille gas storage facility. Figure 2.1 from (Gas_storage_Denmark, 2018)

Figure 3. Well locations and extension of the different gas zones at the Stenlille gas storage facility. Contour lines indicate depth in metres to the top Gassum Formation. Red triangles are the deployed seismographs for the SECURE project. The seismographs in the network are within 5 km of the main pumping station. Modified from figure 2.2 in (Gas_storage_Denmark, 2018)

Figure 4a and b. Dots are locations of seismological events. Blue (earthquakes), light blue (explosions or presumed explosions) and lilac (spurious events) detected by screening the Stenlille stations. Red and grey: Earthquakes and explosions found by the Danish Seismological service in the period Oct. 2018 – March 2020 within the marked box. Triangles are seismological stations. Dark green: Stenlille network. Yellow: Raspberry stations. Light green: permanent stations in national networks. b) stations with observations of the spurious event 2019-12-16 01:23 utc

Figure 5. Spurious event 2019-12-16 01:23 utc ML 0.5 as seen on STE01. The data are unfiltered, and present frequencies of approx. 10 Hz, very low for an event this small.

Figure 6. History of pumping activity at Stenlille gas storage facility. Modified from figure 3.1 in (Gas_storage_Denmark, 2018)

TABLES

Table 1: Locatable events found by the Stenlille monitoring network. LQ is earthquake, LE is confirmed explosion, LP is probable explosion, R is regional event, D is distant earthquake, LX is spurious event (see text).

Table 2 Estimates of detection level of the Stenlille monitoring network



1 Introduction

Monitoring is fundamental to determine whether the injection of fluids in the subsurface is progressing as expected. Microseismic activity can reveal early signs of undesirable consequences of pumping, and monitoring seismicity can be part of an effective mitigation strategy through the Traffic Light System (e.g. (Koppelman et al., 2012 ;De Pater and Baisch, 2011 ;(Green et al., 2012; Porter et al., 2019);Cherry et al., 2014). For a general overview see (Ajayi et al., 2019)

Induced and triggered seismicity are well-known side effects of subsurface activities across a wide range of fields such as hydrocarbon production, gas storage, waste disposal and geothermal energy production. Induced earthquakes are micro-events occurring in the vicinity of injection wells, whereas triggered earthquakes are typically larger events caused by stress changes on nearby faults (e.g. Ellsworth, 2013). Larger earthquakes occurring in connection with production operations are of course unacceptable, as they can cause harm and expensive damage to surface or subsurface infrastructure. Even smaller earthquakes can lead to public concern and resentment, as seen for example in Groningen, the Netherlands (van Thienen-Visser and Breunese, 2015).

On the other hand, microseismic events, which are typically too weak to be felt by the population, are extremely useful for monitoring and mitigation strategies. Microseismic activity near a production site can act as a state-of-health indicator for the subsurface, where a rising level of microseismic activity can be a sign of stress perturbations or pore pressure changes (Ellsworth, 2013). It is important to point out that seismic monitoring cannot serve as the sole monitoring technology. It should be part of a larger monitoring plan encompassing other geophysical, geological and geochemical technologies as outlined in (European_Communities, 2009).

2 The role of baseline monitoring

For the ideal monitoring scenario, the natural seismicity in the area of interest is determined through a baseline monitoring campaign before the onset of subsurface activities. The purpose of the baseline monitoring is to establish the level of natural seismicity in the undisturbed environment, making it possible to identify changes caused by anthropogenic activity. A local network of seismographs is deployed in the area of interest for a period of a few years or more before operations commence (Schoenball et al., 2015; Wilson et al., 2015). The best results are obtained if the baseline monitoring network has the same sensitivity to microseismic events as the monitoring network during operations. If the baseline monitoring network is less sensitive than the operational monitoring network, there is a higher risk of mistaking natural events for anthropogenic events as the level of natural seismicity might be underestimated.

In their simplest form, statistical methods compare the pre-operational baseline seismicity at the location of interest to the seismicity at the same location during operation. If the level of seismicity increases, any additional earthquake will most likely be the result of the operational activities (Ellsworth, 2013; Grigoli et al., 2017). This simple correlation is used in mitigation procedures such as the Traffic Light System (e.g. (Cherry et al., 2014; De Pater and Baisch, 2011; Koppelman et al., 2012). It requires high-precision hypocenter location and preferably also modelling to discriminate between natural and anthropogenic events with a good confidence level.

3 Establishing a post-operational baseline

The recommended best practice will always be to establish a baseline for natural seismicity before operations start, discussed in SECURE D3.1. In some cases, this is not possible because operations have started years or decades back in time, before anyone realized a baseline would be useful. In other cases, there is not enough time to measure a proper robust baseline before operations are scheduled to commence. In these cases, it is necessary to establish the baseline post-operationally.



Tests and descriptions of how to establish a baseline post-operational are virtually absent in literature on induced and triggered seismicity. There is one documented successful example from the Coso Geothermal Field in California, USA described in Schoenball et al. (2015). The Coso site has a high level of natural seismicity as well as strong indications of induced/triggered seismicity. Detailed analysis of the earthquakes in the area revealed that part of the seismicity consisted of earthquake pairs, uncharacteristic of the natural seismicity in the region. The post-operational microseismic baseline at Coso was constructed by measuring in similar geology under a similar tectonic regime and comparing the undisturbed site with the production site. This principle can be transferred to other sites; however, the specific analysis methods may vary.

GEUS has established a post-operational seismicity baseline for the Stenlille Gas Storage Site for the SECURE project. The principles used were similar to the Coso example: a seismicity baseline established in undisturbed conditions on the Gassum Formation near Dybvad, Denmark by GEUS in 2014–2015 (as described in SECURE D3.1) was compared to the post-operational seismicity baseline established on the Gassum Formation at the Stenlille Gas Storage Site. The two baselines are very similar as no earthquakes were detected. Even without earthquakes important lessons were learned from the analysis as described below.

4 The Stenlille gas storage facility

The Stenlille natural gas underground storage facility is located 70 km SW of Copenhagen and has been in operation since 1989 (Fig.1). The storage facility has been re-developed during time in order to increase storage capacity.

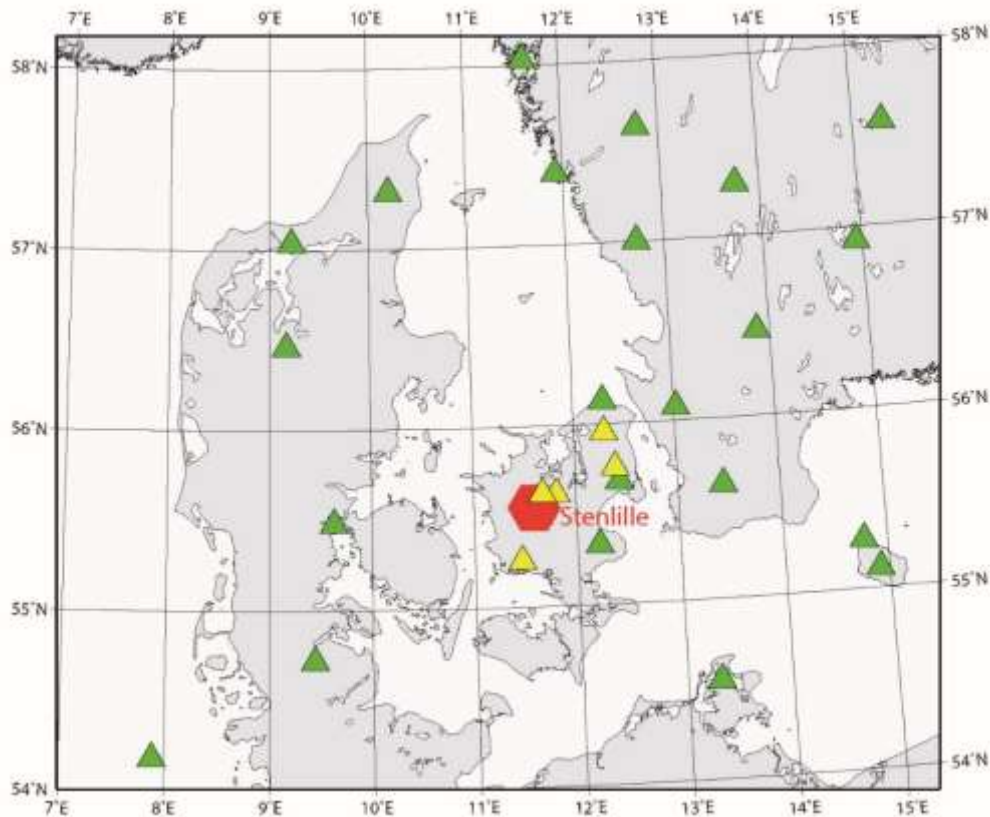


Figure 2. The Stenlille gas storage is located on Sjælland (red hexagon), The triangles are seismicological stations (green – permanent network stations; yellow – additional Raspberry Shake stations deployed and used in this study).



The Stenlille structure is an anticlinal structure shaped by salt tectonics and with a vertical closure of approximate 35 m covering an area of 14 km² (Fig. 2). The Upper Triassic – Lower Jurassic Gassum Sandstone Formation forms the reservoir where gas is stored by displacing formation water. The top Gassum surface is located 1500-1600m below ground in the Stenlille area. The Gassum Formation consists of cyclically interbedded sandstone and marine mudstone layers that were deposited as a result of changes in the depositional environment (Hamberg and Henrik, 2000). The overlying 300 m thick Lower Jurassic Fjerritslev Formation, which consists of claystone, serves as a caprock for the sandstone reservoir.

The total estimated storage capacity of the Stenlille structure equals three billion normal cubic metres, and due to reservoir heterogeneities, gas is stored in several separate zones. The gas storage is at present operated by 14 wells for injection and withdrawal of gas in natural porosity, and six wells used for observational purposes, most of them in the periphery of the structure (Fig. 3). (Laiier and Øbro, 2009).

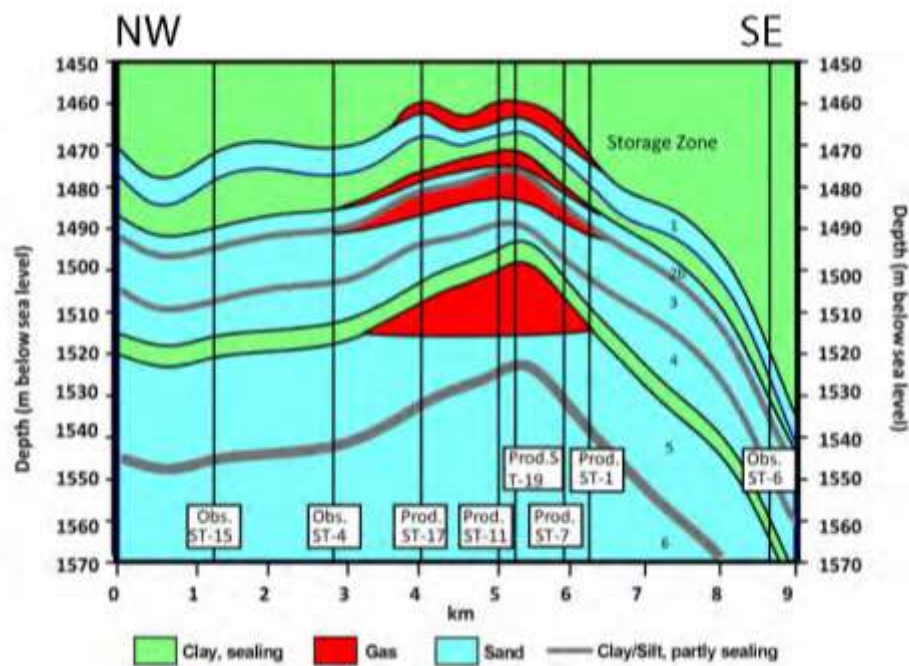


Figure 3 Cross section of the Stenlille gas storage facility. (Fig. 2.1 from Gas_storage_Denmark 2018)

For safety reasons and to protect the environment it is necessary to monitor the storage operation carefully. No sign of gas leakage has been observed in a monitoring well located in a sand stringer 15 m above the gas reservoir. Other monitoring wells have been installed in order to check for possible lateral escape of natural gas.

A pre-operational microseismic baseline monitoring is obviously not possible at active sites. Instead microseismic monitoring around an active site has been combined with baseline measurements in a comparable geological setting at a distance. As this has not been done before, it will be necessary to experiment with baseline instruments in a range of distances from the well/storage facility, between 10 and 100 km, to establish best practice.

4.1 THE STENLILLE POST-OPERATIONAL MICROSEISMIC MONITORING NETWORK

During the period August to September 2018, GEUS established a microseismic monitoring network on the Gassum Formation around the Stenlille gas storage facility (Figure 3). The network consists of 6 seismographs placed within 5 km of the main pumping facility. For the Stenlille network, Nanometrics Trillium seismometers from the DanSeis instrument pool were deployed. Continuous data sampled at 100 Hz are transmitted to GEUS 24/7. In addition, several smaller Raspberry Shake sensors were operated for shorter periods at distances up to 100 km. Permanent stations from the Danish, Swedish and Norwegian seismic monitoring networks were also included, although at larger distances.

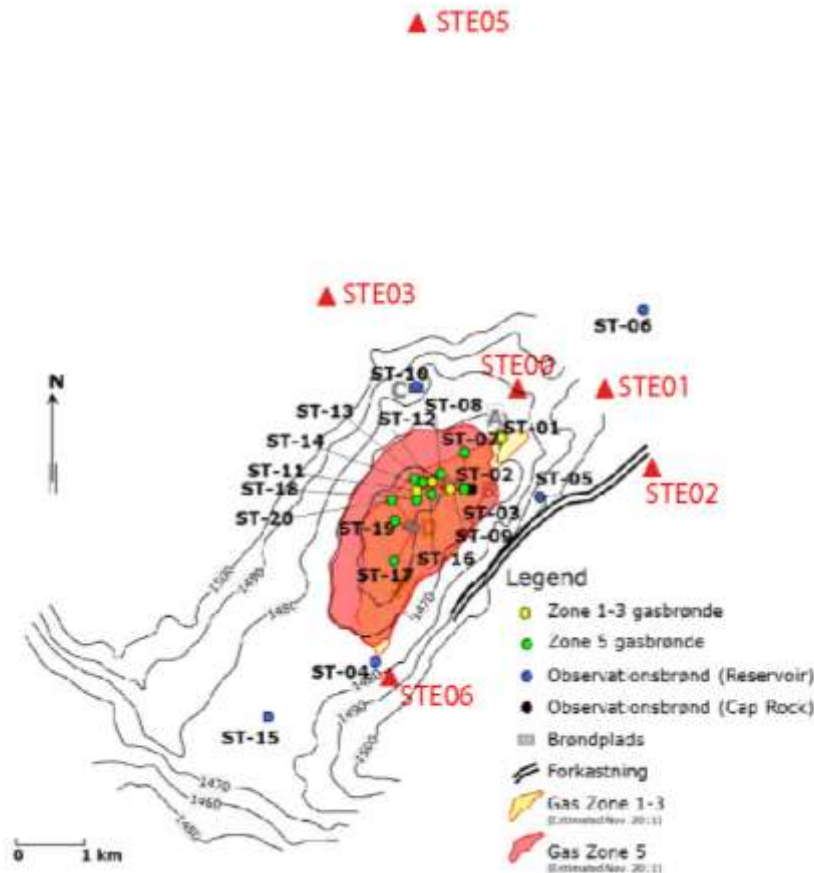


Figure 3. Well locations and extension of the different gas zones at the Stenlille gas storage facility. Contour lines indicate depth in metres to the top Gassum Formation. Red triangles are the deployed seismographs for the SECURE project. The seismographs in the network are within 5 km of the main pumping station. Modified from figure 2.2 in (Gas_storage_Denmark, 2018)

4.2 DATA ANALYSIS

Analysis of the Stenlille data shows a high noise level. One of the original sites (STE04) was quickly abandoned and replaced by another (STE06) due to an unacceptable noise level high above the International High Noise model levels (see for example McNamara and Buland, 2004). The rest of the seismographs have noise levels below the International High Noise Model. Station STE03 is included in the daily screening for events and all stations included in localisation where relevant at the GEUS' seismic service as an extra quality control. The noise analysis is described in more detail in SECURE D 3.1.

4.3 DETECTION OF EVENTS

Data for the period 2018-10-01 to 2020-03-31 have been screened for events, using the CONDET code (see the SEISAN manual: <http://seisan.info/>). The screening triggers several hundred times on the data. The triggers are very unevenly spaced, depending on thunderstorms and noise. A manual screening of the triggered events results in 32 locatable events (Appendix 1) and a large number of acoustic events related to thunderstorms. Of the 32 located events, 20 are previously known events (both natural earthquakes and explosions) which either are fairly close to Stenlille, or large enough and with a frequency content within the range used to trigger



the Stenlille stations alone. Twelve previously unknown and spurious events were found, seen only on the Stenlille network, and a number of similar events which could not be located (spurious events are discussed in the following text). None of the events found are within the Stenlille Gas Storage area. The found events are between ML -0.2 and ML 2.5 (and a distant event Mb6.7 and two regional events of ML 3.5 and ML 2.8); the new spurious events are all under ML 1.0.



Date	time	utc	type	latitude	longitude	depth	n stations	RMS	ML	comment
2018 - 10 - 24	10 : 7		LE	55.056	12.819	0.0F	17	1	1.5	Explosion
2018 - 10 - 26	16 : 23		LQ	56.666	11.733	31.2	15	0.4	2.4	Isefjord
2018 - 10 - 31	10 : 55		LQ	55.775	11.749	7.5	19	0.5	1.4	Isefjord
2018 - 11 - 22	16 : 34		LQ	55.097	15.612	18.6	6	0.3	1.6	Bornholm
2018 - 12 - 4	1 : 31		LQ	55.675	11.760	26.8	13	0.3	1.1	Isefjord
2018 - 11 - 30	14 : 49		LX	55.416	11.524	1.4	3	0.1	0.8	
2018 - 12 - 12	7 : 45		LX	55.450	11.756	0	3	0.4	0.1	
2018 - 12 - 27	9 : 31		LX	55.445	12.007	0	3	0.7	0.7	
2019 - 6 - 19	8 : 0		LE	55.165	12.687	0.0F	15	1	1.7	Explosion
2019 - 8 - 29	6 : 23		LP	54.506	10.979	0.0F	10	0.8	2.6	Probable explosion
2019 - 3 - 21	16 : 31		LQ	55.805	11.801	11.8	14	0.5	1.4	Isefjord
2019 - 12 - 4	4 : 36		LQ	55.760	11.779	18.1	15	0.7	1.9	Isefjord
2019 - 12 - 9	11 : 38		LQ	55.707	12.139	24.8	18	0.9	1.9	Gundsøllille
2019 - 12 - 27	20 : 32		LQ	55.794	11.730	9.6	17	0.7	0.9	Isefjord
2019 - 12 - 27	22 : 20		LQ	56.354	11.148	15.0F	22	1.1	2.4	Off Djursland
2019 - 12 - 7	7 : 23		LX	55.472	11.582	4.6	3	0.1	0.2	
2019 - 12 - 16	1 : 23		LX	55.467	11.410	0	4	0.7	0.5	
2019 - 12 - 21	19 : 24		LX	55.484	11.496	5.6	4	0.1	0.1	
2019 - 12 - 23	8 : 9		LX	55.443	11.630	15	4	0.4	0.6	
2019 - 11 - 30	4 : 58		R	51.514	16.014	0	18	1	2.8	Poland
2019 - 8 - 28	15 : 30		RP	54.299	10.961	1.4	12	0.6	1.6	Probable explosion
2020 - 2 - 13	10 : 33		D	45.924	148.918	0.3	46	0.7	6.7	Distant
2020 - 3 - 9	4 : 46		LP	55.317	13.558	15	4	0.4	1.9	Probable explosion
2020 - 1 - 1	12 : 49		LQ	55.771	11.744	15.5	15	0.5	1.1	Isefjord
2020 - 1 - 13	20 : 41		LQ	55.743	11.709	29.2	24	0.6	1.8	Isefjord
2020 - 1 - 6	0 : 17		LX	55.584	11.515	9.3	3	0.2	-0.2	
2020 - 1 - 10	14 : 46		LX	55.462	11.500	1	3	0.1	-0.1	
2020 - 1 - 27	2 : 38		LX	55.626	12.143	0	4	0.8	1.0	
2020 - 3 - 5	3 : 27		LX	55.432	11.597	0.8	3	0.1	0.4	
2020 - 3 - 17	17 : 46		LX	55.487	11.597	6.7	3	0	0.1	
2020 - 2 - 22	18 : 43		RQ	55.712	2.954	39.9	30	0.6	3.5	North Sea

Table 1: Locatable events found by the Stenlille monitoring network. LQ is earthquake, LE is confirmed explosion, LP is probable explosion, R is regional event, D is distant earthquake, LX is spurious event (see text).

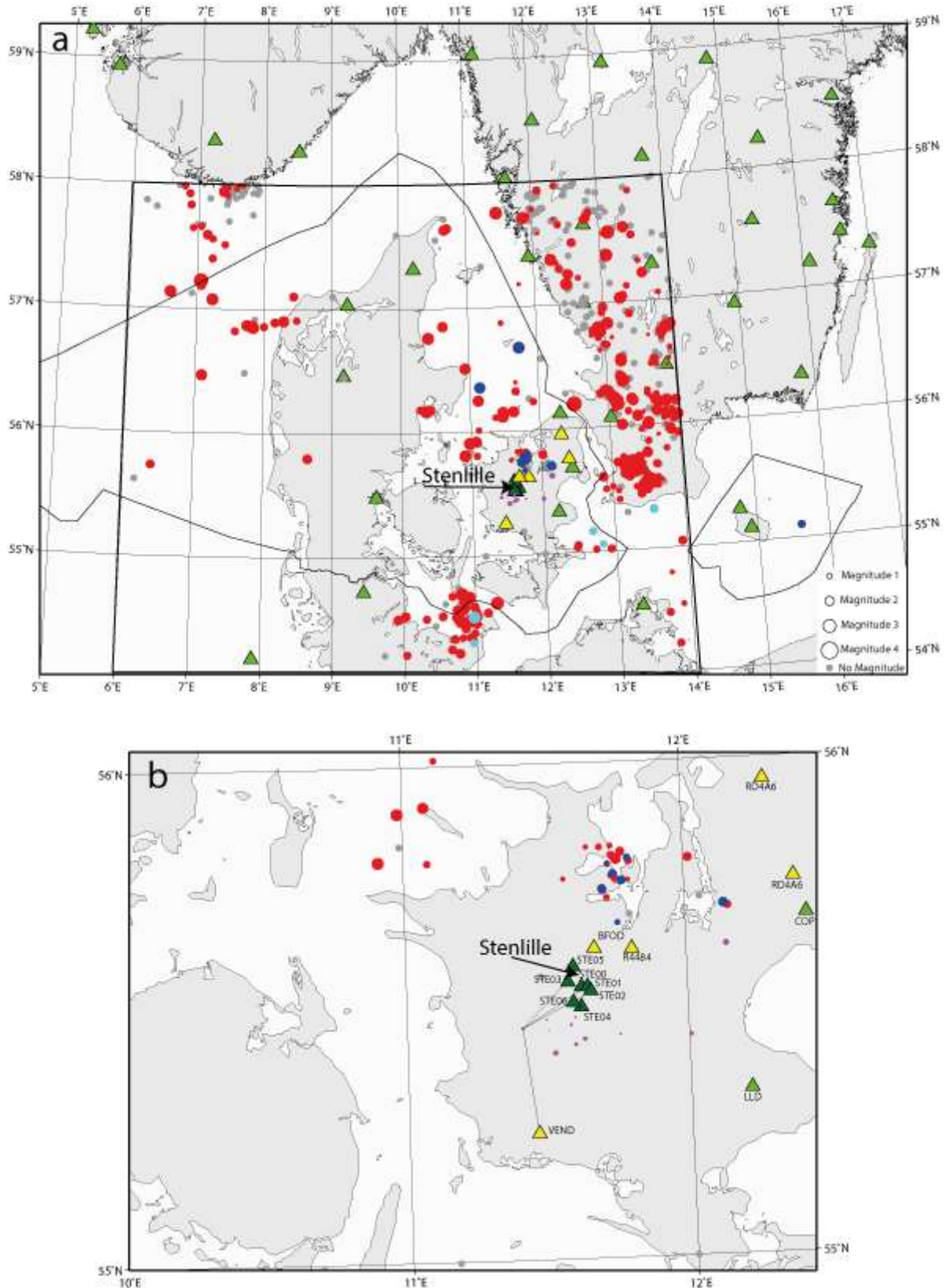


Figure 4a and b. Dots are locations of seismological events. Blue (earthquakes), light blue (explosions or presumed explosions) and lilac (spurious events) detected by screening the Stenlille stations. Red and grey: Earthquakes and explosions detected by the Danish Seismological service in the period Oct. 2018 – March 2020 within the box marked. Triangles are seismological stations. Dark green: Stenlille



network. Yellow: Raspberry stations. Light green: permanent stations in national networks. b) stations with observations of the spurious event 2019-12-16 01:23 utc

The spurious events (lilac in figure 4 and marked LX in table 1):

These events all have magnitudes below 1 (often much smaller) and all have similar signals (Figure 5), with curiously low frequencies of around 10 Hz – much lower than expected for such small events. We do not know what these events are, but in spite of the large uncertainty in the location, we are convinced that they do not originate within the area of the Stenlille gas storage facility, due to the difference in P and S arrival times, corresponding to distances of 10-20 km distance from the stations.

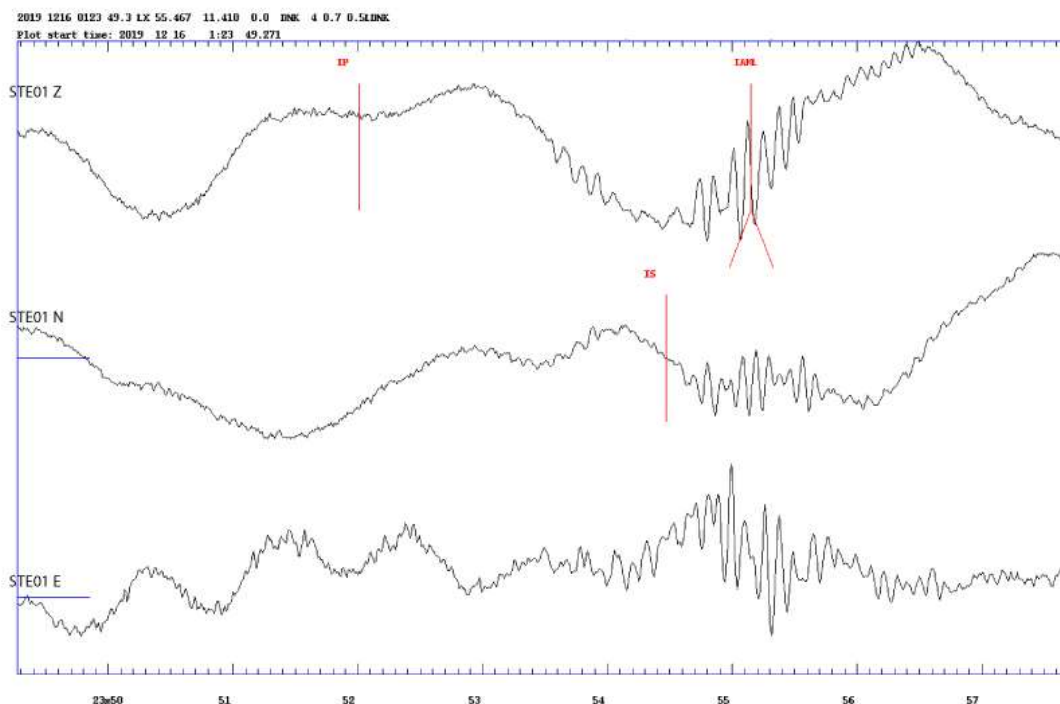


Figure 5. Spurious event 2019-12-16 01:23 utc ML 0.5 as seen on STE01. The data are unfiltered, and present frequencies of approx. 10 Hz, very low for an event this small.

The earthquakes and explosions (blue and light blue in figure 4 and marked LQ, LP or LE in table 1):

These events, detected by screening the Stenlille network, were all previously located by the routine monitoring of the Danish seismic service. The fact that these events were detected by screening only the Stenlille network is an indication that the network is capable of detecting events.

4.4 CORRELATION WITH PUMPING

We have detailed information on the pumping activity at the gas storage facility, but as we see no events in the area, we cannot correlate events with pumping activity.

4.5 DETECTION LEVEL

In order to determine the detection level within the Stenlille gas storage area we have used the 10 natural earthquakes detected by the Stenlille network. The equation for calculating the local magnitude (ML) for earthquakes in Denmark is $ML = 0.925 \cdot \log_{10}(A) + 1.61 \log_{10}(\Delta) - 2.38$ (Gregersen, 1999) where A is the maximum amplitude of the S and surface wave arrival train in nm and Δ is the distance in km. Observe that the equations for ML are different for different areas.



If we assume that actual observed amplitudes for each of the 10 earthquakes originate from events closer to Stenlille, we obtain a series of estimates of which magnitudes it would be possible to see if the events occurred within the Stenlille gas storage facility.

The equation for ML used is not verified for distances below 1 degree of distance, but is the best available. This means that the results must be interpreted as the best available estimate. The complete set of calculations are included in Appendix 1. The average values for all earthquakes and stations are shown in Table 2.

Distance (km)	1	2	3	4	5	6	7	8	9	10
Average ML observable	-1.2	-0.7	-0.4	-0.2	0.0	0.1	0.2	0.3	0.4	0.4

Table 2 Estimates of detection level of the Stenlille monitoring network

We estimate the detection level of the Stenlille network for events within the gas storage facility to be at least M0.0.

5 Discussion of results – why do we not see any events at Stenlille?

The Stenlille monitoring network has not registered any seismic events within the Stenlille gas storage facility through 18 months of monitoring. The detection level is estimated to be at or below M0.0, meaning that any events that have not been detected are very small.

GEUS has monitored earthquakes in Denmark for many years, and no earthquake has ever been located at Stenlille, bearing in mind the detection level for national monitoring network for onshore Denmark up to ML 2.0 (Dahl-Jensen et al., 2013; Voss et al., 2015). The Gas storage facility has been in operation since 1989, pumping up to $500 \times 10^6 \text{ m}^3$ of gas in and out (Figure 6) and has to our knowledge never received a complaint about tremors.

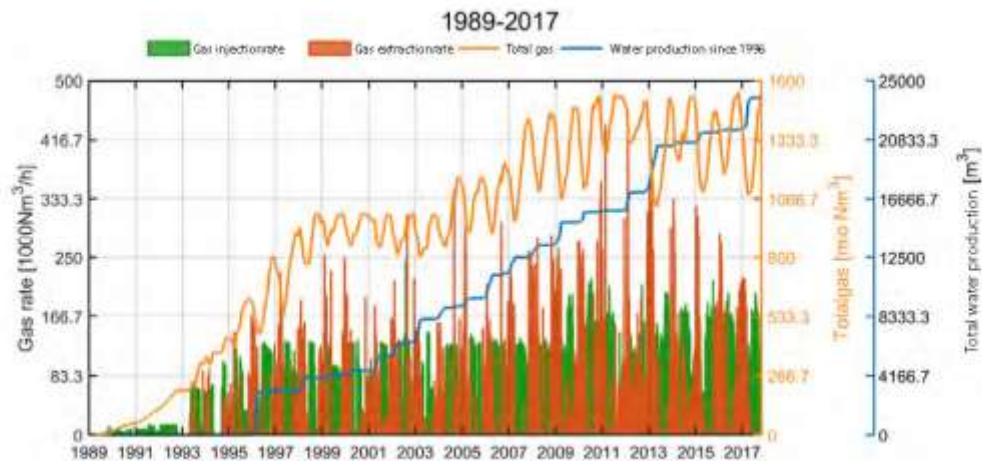


Figure 6. History of pumping activity at Stenlille gas storage facility. Modified from figure 3.1 in (Gas_storage_Denmark, 2018)

We do not know the reason for the absence of events. Of course, events below our detection level could be occurring. We can speculate that during the operation of the monitoring network, after almost 30 years of pumping, all stresses have long since been relieved, and events did occur early in the storage's life. Alternatively it is possible that the stresses in the subsurface (both of natural and anthropogenic origin) are too small to trigger earthquakes.

6 Choosing the optimal network

Choosing the optimal monitoring network is always a balance of quality and cost. The first step is to determine the acceptable level of microseismicity in the location of interest. This decision rests on both scientific knowledge (e.g., understanding of local risk, local geological conditions- presence of faults, subsurface stress regime, shallow geological conditions) and political considerations (e.g., site safety, avoidance of public nuisance, optimizing operational parameters). The second step is to perform a site survey to establish the signal-to-noise conditions and calculate the required network density and configuration to obtain the desired detection level. The detection level is key to be able to mitigate before the acceptable level of microseismicity is exceeded. The third step involves deciding the level of network redundancy in case one or more seismograph stations fail. It is also important to decide the level of network maintenance and data analysis.

7 Discriminating between natural seismicity and anthropogenic seismicity

Discriminating between natural earthquakes and induced/triggered earthquakes is not trivial (overview in Grigoli et al., 2017). Calculating a precise hypocenter and focal mechanism for each earthquake is very useful; however, this is often not possible for small events. High noise in part caused by production activities, insufficient seismograph coverage, and poor velocity models are common obstacles for a comprehensive physics-based analysis. A high-quality baseline is very helpful for discriminating between natural and anthropogenic seismicity. In areas with high levels of seismicity, be it natural or otherwise, statistical methods are useful (Schoenball et al., 2015). With fewer earthquakes it is necessary to apply sophisticated earthquake location and analysis methods to determine the nature of an event, see for example (Lomax et al., 2009; Lomax et al., 2000)



8 Conclusion

Best practice for monitoring induced and triggered seismicity depends to a high degree on local conditions, but in all cases establishing a high-quality pre-operational baseline is recommended. During operations, a local network should be deployed for monitoring and mitigation purposes. If the Traffic Light System is used as a mitigation tool, it is important that the monitoring network has a detection level way below the acceptable level of microseismicity as determined by authorities. No level has been set at Stenlille.

The monitoring network at Stenlille, in operation since summer 2018, has not detected any events within the Stenlille gas storage facility, but did detect other events further away, allowing an estimate of the detection level within the gas storage area.



9 References

- Ajayi, T., Gomes, J. S., and Bera, A., 2019, A review of CO₂ storage in geological formations emphasizing modeling, monitoring and capacity estimation approaches: *Petroleum Science*, p. 1-36.
- Cherry, J., Ben-Eli, M., Bharadwaj, L., Chalaturnyk, R., Dusseault, M. B., Goldstein, B., Lacoursière, J.-P., Matthews, R., Mayer, B., and Molson, J., 2014, Environmental Impacts of Shale Gas Extraction in Canada. The Expert Panel on Harnessing Science and Technology to Understand the Environmental Impacts of Shale Gas Extraction, Ottawa: Council of Canadian Academies.
- Dahl-Jensen, T., Voss, P. H., Larsen, T. B., and Gregersen, S., 2013, Seismic activity in Denmark: detection level and recent felt earthquakes: . *Geological Survey of Denmark and Greenland Bulletin*, v. 28, p. 41-44.
- De Pater, C., and Baisch, S., 2011, Geomechanical study of Bowland Shale seismicity: Synthesis Report, p. 57.
- Ellsworth, W. L., 2013, Injection-Induced Earthquakes: *Science*, v. 341, no. 6142, p. 1-6.
- European Communities, 2009, Directive 2009/31/EC of the European Parliament and the Council of 23 April 2009 on the geological storage of carbon dioxide and amending Council Directive 85/337/EEC, European Parliament and Council Directives 2000/60/EC, 2001/80/EC, 2004/35/EC, 2006/12/EC, 2008/1/EC and Regulation (EC) No 1013/2006.
- Gas_storage_Denmark, 2018, Stenlille gaslager - Undergrunden Årsrapport 2017: Gas Storage Denmark.
- Green, C. A., Styles, P., and Baptie, B. J., 2012, Preese Hall shale gas fracturing review and recommendations for induced seismic mitigation.
- Gregersen, S., 1999, National Survey and Cadastre (KMS), Copenhagen, Denmark, EMSC-CSEM Newsletter, Volume 15, European - Mediterranean Seismological Centre.
- Grigoli, F., Cesca, S., Priolo, E., Rinaldi, A. P., Clinton, J. F., Stabile, T. A., Dost, B., Fernandez, M. G., Wiemer, S., and Dahm, T. J. R. o. G., 2017, Current challenges in monitoring, discrimination, and management of induced seismicity related to underground industrial activities: A European perspective, v. 55, no. 2, p. 310-340.
- Hamberg, L., and Henrik, N. L., 2000, IDansk Olie-& Naturgas A/S, Agern Alle 24-26, DK-2970 Hørsholm, Denmark (e-mail: ham@ dopas. dk) 2Geological Survey of Denmark and Greenland (GEUS), Thoravej 8, DK-2400 Copenhagen NV, Denmark: Sedimentary Responses to Forced Regressions, v. 172, p. 69.
- Koppelman, B., Walker, A., and Woods, E., 2012, Shale gas extraction in the UK: a review of hydraulic fracturing, The Royal Society, The Royal Academy of Engineering.
- Laier, T., and Øbro, H., 2009, Environmental and safety monitoring of the natural gas underground storage at Stenlille, Denmark: Geological Society, London, Special Publications, v. 313, no. 1, p. 81-92.
- Lomax, A., Michelini, A., and Curtis, A., 2009, Earthquake location, direct, global-search methods: *Encyclopedia of complexity and system science*, v. 5, p. 1-33.
- Lomax, A., Virieux, J., Volant, P., and Berge-Thierry, C., 2000, Probabilistic earthquake location in 3D and layered models, *Advances in seismic event location*, Springer, p. 101-134.
- McNamara, D. E., and Buland, R. P., 2004, Ambient Noise Levels in the Continental United States: *Bulletin of the Seismological Society of America*, v. 94, no. 4, p. 1517-1527.
- Porter, R. T., Striolo, A., Mahgerefteh, H., and Faure Walker, J., 2019, Addressing the risks of induced seismicity in subsurface energy operations: *Wiley Interdisciplinary Reviews: Energy and Environment*, v. 8, no. 2, p. e324.
- Schoenball, M., Davatzes, N. C., and Glen, J. M. J. G. R. L., 2015, Differentiating induced and natural seismicity using space-time-magnitude statistics applied to the Coso Geothermal field, v. 42, no. 15, p. 6221-6228.
- van Thienen-Visser, K., and Breunese, J., 2015, Induced seismicity of the Groningen gas field: History and recent developments: *The Leading Edge*, v. 34, no. 6, p. 664-671.
- Voss, P., Dahl-Jensen, T., and Larsen, T. B., 2015, Earthquake Hazard in Denmark: Geological Survey of Denmark and Greenland report, v. 2015/24, p. pp 53.
- Wilson, M. P., Davies, R. J., Foulger, G. R., Julian, B. R., Styles, P., Gluyas, J. G., Almond, S. J. M., and Geology, P., 2015, Anthropogenic earthquakes in the UK: A national baseline prior to shale exploitation, v. 68, p. 1-17.



Appendix 1

For each of the natural, local earthquakes detected by the Stenlille monitoring network, the amplitude used in determining the local magnitude (ML) at each station is noted. Then, using the equation for ML, the same amplitude is used assuming distances of 1 – 10 km from the each Stenlille to calculate the corresponding assumed ML.

$$ML = 0.925 \cdot \log_{10}(A) + 1.61 \log_{10}(\Delta) - 2.38 \text{ (Gregersen, 1999)}$$

The equation for ML for Denmark is not verified for distances below 1 degree of distance, but is the best available. This means that the results must be interpreted as the best available estimate.



$$ML = 0.925 * \log_{10}(Anm) + 1.61 \log_{10}(\Delta) - 2.38$$

2018-10-26 16:23 LQ ML 2.4

	distance	ampl	period	magnitude
STE01	128.9	19.5	0.1	2.2
	10	19.5	0.1	0.4
	9	19.5	0.1	0.3
	8	19.5	0.1	0.3
	7	19.5	0.1	0.2
	6	19.5	0.1	0.1
	5	19.5	0.1	-0.1
	4	19.5	0.1	-0.2
	3	19.5	0.1	-0.4
	2	19.5	0.1	-0.7
	1	19.5	0.1	-1.2

	distance	ampl	period	magnitude
STE02	129.9	30	0.2	2.4
	10	30	0.2	0.6
	9	30	0.2	0.5
	8	30	0.2	0.4
	7	30	0.2	0.3
	6	30	0.2	0.2
	5	30	0.2	0.1
	4	30	0.2	0.0
	3	30	0.2	-0.2
	2	30	0.2	-0.5
	1	30	0.2	-1.0

	distance	ampl	period	magnitude
STE03	127.9	39.9	0.3	2.5
	10	39.9	0.3	0.7
	9	39.9	0.3	0.6
	8	39.9	0.3	0.6
	7	39.9	0.3	0.5
	6	39.9	0.3	0.4
	5	39.9	0.3	0.2
	4	39.9	0.3	0.1
	3	39.9	0.3	-0.1
	2	39.9	0.3	-0.4
	1	39.9	0.3	-0.9

	distance	ampl	period	magnitude
STE05	124	56.6	0.3	2.6
	10	56.6	0.3	0.9
	9	56.6	0.3	0.8
	8	56.6	0.3	0.7
	7	56.6	0.3	0.6
	6	56.6	0.3	0.5

5	56.6	0.3	0.4
4	56.6	0.3	0.2
3	56.6	0.3	0.0
2	56.6	0.3	-0.3
1	56.6	0.3	-0.8

	distance	ampl	period	magnitude
STE06	131.8	16.6	0.2	2.2
	10	16.6	0.2	0.4
	9	16.6	0.2	0.3
	8	16.6	0.2	0.2
	7	16.6	0.2	0.1
	6	16.6	0.2	0.0
	5	16.6	0.2	-0.1
	4	16.6	0.2	-0.3
	3	16.6	0.2	-0.5
	2	16.6	0.2	-0.8
	1	16.6	0.2	-1.3

2018-10-31 10:55 LQ ML 1.4

	distance	ampl	period	magnitude
STE01	27.2	16.4	0.14	1.1
	10	16.4	0.14	0.4
	9	16.4	0.14	0.3
	8	16.4	0.14	0.2
	7	16.4	0.14	0.1
	6	16.4	0.14	0.0
	5	16.4	0.14	-0.1
	4	16.4	0.14	-0.3
	3	16.4	0.14	-0.5
	2	16.4	0.14	-0.8
	1	16.4	0.14	-1.3

	distance	ampl	period	magnitude
STE02	27.9	16.6	0.2	1.1
	10	16.6	0.2	0.4
	9	16.6	0.2	0.3
	8	16.6	0.2	0.2
	7	16.6	0.2	0.1
	6	16.6	0.2	0.0
	5	16.6	0.2	-0.1
	4	16.6	0.2	-0.3
	3	16.6	0.2	-0.5
	2	16.6	0.2	-0.8
	1	16.6	0.2	-1.3

	distance	ampl	period	magnitude
STE03	27.5	28.2	0.18	1.3
	10	28.2	0.18	0.6
	9	28.2	0.18	0.5
	8	28.2	0.18	0.4
	7	28.2	0.18	0.3
	6	28.2	0.18	0.2
	5	28.2	0.18	0.1
	4	28.2	0.18	-0.1
	3	28.2	0.18	-0.3
	2	28.2	0.18	-0.6
	1	28.2	0.18	-1.0

	distance	ampl	period	magnitude
STE06	31.5	11.6	0.18	1.0
	10	11.6	0.18	0.2
	9	11.6	0.18	0.1
	8	11.6	0.18	0.1
	7	11.6	0.18	0.0
	6	11.6	0.18	-0.1

5	11.6	0.18	-0.3
4	11.6	0.18	-0.4
3	11.6	0.18	-0.6
2	11.6	0.18	-0.9
1	11.6	0.18	-1.4

2018-12-04 01:31 LQ ML 1.1

	distance	ampl	period	magnitude
STE01	31.2	4.4	0.14	0.6
	10	4.4	0.14	-0.2
	9	4.4	0.14	-0.2
	8	4.4	0.14	-0.3
	7	4.4	0.14	-0.4
	6	4.4	0.14	-0.5
	5	4.4	0.14	-0.7
	4	4.4	0.14	-0.8
	3	4.4	0.14	-1.0
	2	4.4	0.14	-1.3
	1	4.4	0.14	-1.8

	distance	ampl	period	magnitude
STE02	31.5	5.6	0.2	0.7
	10	5.6	0.2	-0.1
	9	5.6	0.2	-0.2
	8	5.6	0.2	-0.2
	7	5.6	0.2	-0.3
	6	5.6	0.2	-0.4
	5	5.6	0.2	-0.6
	4	5.6	0.2	-0.7
	3	5.6	0.2	-0.9
	2	5.6	0.2	-1.2
	1	5.6	0.2	-1.7

	distance	ampl	period	magnitude
STE03	32	9.3	0.2	0.9
	10	9.3	0.2	0.1
	9	9.3	0.2	0.1
	8	9.3	0.2	0.0
	7	9.3	0.2	-0.1
	6	9.3	0.2	-0.2
	5	9.3	0.2	-0.4
	4	9.3	0.2	-0.5
	3	9.3	0.2	-0.7
	2	9.3	0.2	-1.0
	1	9.3	0.2	-1.5

	distance	ampl	period	magnitude
STE05	30.3	8.4	0.2	0.9
	10	8.4	0.2	0.1
	9	8.4	0.2	0.0
	8	8.4	0.2	-0.1
	7	8.4	0.2	-0.2
	6	8.4	0.2	-0.3

5	8.4	0.2	-0.4
4	8.4	0.2	-0.6
3	8.4	0.2	-0.8
2	8.4	0.2	-1.0
1	8.4	0.2	-1.5

	distance	ampl	period	magnitude
STE06	33.7	4.9	0.2	0.7
	10	4.9	0.2	-0.1
	9	4.9	0.2	-0.2
	8	4.9	0.2	-0.3
	7	4.9	0.2	-0.4
	6	4.9	0.2	-0.5
	5	4.9	0.2	-0.6
	4	4.9	0.2	-0.8
	3	4.9	0.2	-1.0
	2	4.9	0.2	-1.3
	1	4.9	0.2	-1.7

2019-03-21 16:31 LQ ML 1.4

	distance	ampl	period	magnitude
STE01	32.5	24.3	0.3	1.3
	10	24.3	0.3	0.5
	9	24.3	0.3	0.4
	8	24.3	0.3	0.4
	7	24.3	0.3	0.3
	6	24.3	0.3	0.2
	5	24.3	0.3	0.0
	4	24.3	0.3	-0.1
	3	24.3	0.3	-0.3
	2	24.3	0.3	-0.6
	1	24.3	0.3	-1.1

	distance	ampl	period	magnitude
STE02	33.2	17.7	0.2	1.2
	10	17.7	0.2	0.4
	9	17.7	0.2	0.3
	8	17.7	0.2	0.2
	7	17.7	0.2	0.1
	6	17.7	0.2	0.0
	5	17.7	0.2	-0.1
	4	17.7	0.2	-0.3
	3	17.7	0.2	-0.5
	2	17.7	0.2	-0.7
	1	17.7	0.2	-1.2

	distance	ampl	period	magnitude
STE03	33.1	22.3	0.2	1.3
	10	22.3	0.2	0.5
	9	22.3	0.2	0.4
	8	22.3	0.2	0.3
	7	22.3	0.2	0.2
	6	22.3	0.2	0.1
	5	22.3	0.2	0.0
	4	22.3	0.2	-0.2
	3	22.3	0.2	-0.4
	2	22.3	0.2	-0.6
	1	22.3	0.2	-1.1

	distance	ampl	period	magnitude
STE05	29.7	45.7	0.3	1.5
	10	45.7	0.3	0.8
	9	45.7	0.3	0.7
	8	45.7	0.3	0.6
	7	45.7	0.3	0.5
	6	45.7	0.3	0.4

5	45.7	0.3	0.3
4	45.7	0.3	0.1
3	45.7	0.3	-0.1
2	45.7	0.3	-0.4
1	45.7	0.3	-0.8

	distance	ampl	period	magnitude
STE06	36.7	12.7	0.4	1.2
	10	12.7	0.4	0.3
	9	12.7	0.4	0.2
	8	12.7	0.4	0.1
	7	12.7	0.4	0.0
	6	12.7	0.4	-0.1
	5	12.7	0.4	-0.2
	4	12.7	0.4	-0.4
	3	12.7	0.4	-0.6
	2	12.7	0.4	-0.9
	1	12.7	0.4	-1.4

2019-12-27 20:32 LQ ML 0.9

	distance	ampl	period	magnitude	
STE01	27.9		5.9	0.06	0.7
	10		5.9	0.06	-0.1
	9		5.9	0.06	-0.1
	8		5.9	0.06	-0.2
	7		5.9	0.06	-0.3
	6		5.9	0.06	-0.4
	5		5.9	0.06	-0.5
	4		5.9	0.06	-0.7
	3		5.9	0.06	-0.9
	2		5.9	0.06	-1.2
	1		5.9	0.06	-1.7

STE02	28.7		8.2	0.24	0.8
	10		8.2	0.24	0.1
	9		8.2	0.24	0.0
	8		8.2	0.24	-0.1
	7		8.2	0.24	-0.2
	6		8.2	0.24	-0.3
	5		8.2	0.24	-0.4
	4		8.2	0.24	-0.6
	3		8.2	0.24	-0.8
	2		8.2	0.24	-1.1
	1		8.2	0.24	-1.5

STE03 distance ampl period magnitude

STE05 distance ampl period magnitude

	distance	ampl	period	magnitude
STE06	32	12.9	0.09	1.1
	10	12.9	0.09	0.3
	9	12.9	0.09	0.2
	8	12.9	0.09	0.1
	7	12.9	0.09	0.0
	6	12.9	0.09	-0.1
	5	12.9	0.09	-0.2
	4	12.9	0.09	-0.4
	3	12.9	0.09	-0.6
	2	12.9	0.09	-0.9
	1	12.9	0.09	-1.4

2019-12-27 22_20 LQ ML 2.4

	distance	ampl	period	magnitude
STE01	94.9	95.6	0.5	2.7
	10	95.6	0.5	1.1
	9	95.6	0.5	1.0
	8	95.6	0.5	0.9
	7	95.6	0.5	0.8
	6	95.6	0.5	0.7
	5	95.6	0.5	0.6
	4	95.6	0.5	0.4
	3	95.6	0.5	0.2
	2	95.6	0.5	-0.1
	1	95.6	0.5	-0.5

STE02	96	50	0.14	2.4
	10	50	0.14	0.8
	9	50	0.14	0.7
	8	50	0.14	0.6
	7	50	0.14	0.6
	6	50	0.14	0.4
	5	50	0.14	0.3
	4	50	0.14	0.2
	3	50	0.14	0.0
	2	50	0.14	-0.3
	1	50	0.14	-0.8

STE03 distance ampl period magnitude

	distance	ampl	period	magnitude
STE05	89.5	96.2	0.14	2.6
	10	96.2	0.14	1.1
	9	96.2	0.14	1.0
	8	96.2	0.14	0.9
	7	96.2	0.14	0.8
	6	96.2	0.14	0.7

5	96.2	0.14	0.6
4	96.2	0.14	0.4
3	96.2	0.14	0.2
2	96.2	0.14	-0.1
1	96.2	0.14	-0.5

	distance	ampl	period	magnitude
STE06	97.2	57.1	0.16	2.4
	10	57.1	0.16	0.9
	9	57.1	0.16	0.8
	8	57.1	0.16	0.7
	7	57.1	0.16	0.6
	6	57.1	0.16	0.5
	5	57.1	0.16	0.4
	4	57.1	0.16	0.2
	3	57.1	0.16	0.0
	2	57.1	0.16	-0.3
	1	57.1	0.16	-0.8

2020-01-01 12:49 LQ 1.4

	distance	ampl	period	magnitude
STE01	25.6	4	0.09	0.5
	10	4	0.09	-0.2
	9	4	0.09	-0.3
	8	4	0.09	-0.4
	7	4	0.09	-0.5
	6	4	0.09	-0.6
	5	4	0.09	-0.7
	4	4	0.09	-0.9
	3	4	0.09	-1.1
	2	4	0.09	-1.3
	1	4	0.09	-1.8

STE02	26.4	13.2	0.09	0.9
	10	13.2	0.09	0.3
	9	13.2	0.09	0.2
	8	13.2	0.09	0.1
	7	13.2	0.09	0.0
	6	13.2	0.09	-0.1
	5	13.2	0.09	-0.2
	4	13.2	0.09	-0.4
	3	13.2	0.09	-0.6
	2	13.2	0.09	-0.9
	1	13.2	0.09	-1.3

STE03 distance ampl period magnitude

STE05 distance ampl period magnitude

	distance	ampl	period	magnitude
STE06	29.9	14.5	0.08	1.1
	10	14.5	0.08	0.3
	9	14.5	0.08	0.2
	8	14.5	0.08	0.1
	7	14.5	0.08	0.1
	6	14.5	0.08	-0.1
	5	14.5	0.08	-0.2
	4	14.5	0.08	-0.3
	3	14.5	0.08	-0.5
	2	14.5	0.08	-0.8
	1	14.5	0.08	-1.3

2020-01-13 20:41 LQ ML 1.8

	distance	ampl	period	magnitude
STE01	22.1	30.9	0.08	1.2
	10	30.9	0.08	0.6
	9	30.9	0.08	0.5
	8	30.9	0.08	0.5
	7	30.9	0.08	0.4
	6	30.9	0.08	0.3
	5	30.9	0.08	0.1
	4	30.9	0.08	0.0
	3	30.9	0.08	-0.2
	2	30.9	0.08	-0.5
	1	30.9	0.08	-1.0

STE02	23	41.5	0.11	1.3
	10	41.5	0.11	0.7
	9	41.5	0.11	0.7
	8	41.5	0.11	0.6
	7	41.5	0.11	0.5
	6	41.5	0.11	0.4
	5	41.5	0.11	0.2
	4	41.5	0.11	0.1
	3	41.5	0.11	-0.1
	2	41.5	0.11	-0.4
	1	41.5	0.11	-0.9

STE03 distance ampl period magnitude

	distance	ampl	period	magnitude
STE05	18.6	60.6	0.09	1.3
	10	60.6	0.09	0.9
	9	60.6	0.09	0.8
	8	60.6	0.09	0.7
	7	60.6	0.09	0.6
	6	60.6	0.09	0.5

5	60.6	0.09	0.4
4	60.6	0.09	0.2
3	60.6	0.09	0.0
2	60.6	0.09	-0.2
1	60.6	0.09	-0.7

distance ampl period magnitude

STE06

2018-11-30 16:34 LQ ML 1.6

	distance	ampl	period	magnitude
STE01				

STE02

STE03	distance	ampl	period	magnitude
	261	11.09	0.12	2.5
	10	11.09	0.12	0.2
	9	11.09	0.12	0.1
	8	11.09	0.12	0.0
	7	11.09	0.12	-0.1
	6	11.09	0.12	-0.2
	5	11.09	0.12	-0.3
	4	11.09	0.12	-0.4
	3	11.09	0.12	-0.6
	2	11.09	0.12	-0.9
	1	11.09	0.12	-1.4

	distance	ampl	period	magnitude
STE05				

STE06 distance ampl period magnitude

2019-12-09 11:38 LQ ML 1.9

	distance	ampl	period	magnitude	average
STE01	43.6	21.8	0.78	1.5	
	10	21.8	0.78	0.5	0.3
	9	21.8	0.78	0.4	0.3
	8	21.8	0.78	0.3	0.2
	7	21.8	0.78	0.2	0.1
	6	21.8	0.78	0.1	0.0
	5	21.8	0.78	0.0	-0.2
	4	21.8	0.78	-0.2	-0.3
	3	21.8	0.78	-0.4	-0.5
	2	21.8	0.78	-0.7	-0.8
	1	21.8	0.78	-1.1	-1.3

	distance	ampl	period	magnitude	
STE02	43.5	25.9	0.1	1.6	
	10	25.9	0.1	0.5	0.4
	9	25.9	0.1	0.5	0.3
	8	25.9	0.1	0.4	0.3
	7	25.9	0.1	0.3	0.2
	6	25.9	0.1	0.2	0.1
	5	25.9	0.1	0.1	-0.1
	4	25.9	0.1	-0.1	-0.2
	3	25.9	0.1	-0.3	-0.4
	2	25.9	0.1	-0.6	-0.7
	1	25.9	0.1	-1.1	-1.2

	distance	ampl	period	magnitude	
STE03					0.4
					0.3
					0.3
					0.2
					0.1
					-0.1
					-0.2
					-0.4
					-0.7
					-1.2

	distance	ampl	period	magnitude	
STE05	44.3	68	0.8	2.0	
	10	68	0.8	0.9	0.7
	9	68	0.8	0.9	0.6
	8	68	0.8	0.8	0.5
	7	68	0.8	0.7	0.4
	6	68	0.8	0.6	0.3

5	68	0.8	0.4	0.2
4	68	0.8	0.3	0.0
3	68	0.8	0.1	-0.2
2	68	0.8	-0.2	-0.4
1	68	0.8	-0.7	-0.9

	distance	ampl	period	magnitude	
STE06	47.4	53.2	0.3	1.9	
	10	53.2	0.3	0.8	0.4
	9	53.2	0.3	0.8	0.3
	8	53.2	0.3	0.7	0.2
	7	53.2	0.3	0.6	0.1
	6	53.2	0.3	0.5	0.0
	5	53.2	0.3	0.3	-0.1
	4	53.2	0.3	0.2	-0.3
	3	53.2	0.3	0.0	-0.5
	2	53.2	0.3	-0.3	-0.7
	1	53.2	0.3	-0.8	-1.2

distance	average
10	0.4
9	0.4
8	0.3
7	0.2
6	0.1
5	0.0
4	-0.2
3	-0.4
2	-0.7
1	-1.2